



Faculty Scholarship

2005

Wave Front Interaction Model of Stabilized Propagating Wave Segments

Vladimir S. Zykov

Kenneth Showalter

Follow this and additional works at: https://researchrepository.wvu.edu/faculty_publications

Digital Commons Citation

Zykov, Vladimir S. and Showalter, Kenneth, "Wave Front Interaction Model of Stabilized Propagating Wave Segments" (2005). *Faculty Scholarship*. 432.

https://researchrepository.wvu.edu/faculty_publications/432

This Article is brought to you for free and open access by The Research Repository @ WVU. It has been accepted for inclusion in Faculty Scholarship by an authorized administrator of The Research Repository @ WVU. For more information, please contact ian.harmon@mail.wvu.edu.

Wave Front Interaction Model of Stabilized Propagating Wave Segments

Vladimir S. Zykov¹ and Kenneth Showalter²

¹*Institut für Theoretische Physik, Technische Universität Berlin, D-10623 Berlin, Germany,*

²*Department of Chemistry, West Virginia University, Morgantown, WV 26506-6045, USA*

(Received 14 July 2004; published 14 February 2005)

A wave front interaction model is developed to describe the relationship between excitability and the size and shape of stabilized wave segments in a broad class of weakly excitable media. These wave segments of finite size are unstable but can be stabilized by feedback to the medium excitability; they define a separatrix between spiral wave behavior and contracting wave segments. Unbounded wave segments (critical fingers) lie on the asymptote of this separatrix, defining the boundary between excitable and subexcitable media. The model predictions are compared with results from numerical simulations.

DOI: 10.1103/PhysRevLett.94.068302

PACS numbers: 82.40.Bj, 05.45.-a, 05.65.+b, 47.54.+r

Wave front interaction models have been developed to describe steadily rotating spiral waves [1] and, in weakly excitable media, critical fingers [2]. Critical fingers are observed at the excitability boundary between excitable and subexcitable media. Both the spiral wavelength and the size of the spiral core increase as excitability decreases in an excitable medium, until, at the excitable-subexcitable boundary, they become infinite. At this critical excitability, the unbounded spiral wave has opened up to form an unbounded, nearly planar wave with a free end, which is the critical finger [3]. At lower excitabilities, in the subexcitable regime, this wave contracts tangentially at its free end. Hakim and Karma have reviewed applications of front interaction models to describe spiral waves and critical fingers [4].

Recent studies of the photosensitive Belousov-Zhabotinsky (BZ) reaction [5,6] have shown that, in addition to spiral waves and critical fingers, there is another possible waveform with a free end, a propagating wave segment that is stationary in size and shape [7–9]. These constant velocity waves have two free ends, and their size and shape are uniquely determined by the excitability of the medium. They are inherently unstable, but they can be easily stabilized by applying an appropriate feedback to the excitability of the medium. Figure 1 shows examples of stabilized wave segments in the photosensitive BZ reaction at two different excitabilities [7,8].

These waves were stabilized by varying the illumination intensity imposed on the reaction medium (thereby varying the excitability) in proportion to the wave size. The locus of wave size as a function of excitability defines a separatrix that delineates the boundary between spiral wave behavior and contracting wave segments. For a particular excitability, there is an unstable wave segment with a particular size (and shape), which, in the absence of stabilizing feedback, will either form counterrotating spiral waves or contract tangentially at its free ends and eventually disappear. The asymptote of the locus of wave size as a function of excitability, where the wave size is infinite, is exactly the same excitability boundary between excit-

able and subexcitable media as defined by the critical finger [7,8].

We note that similar particlelike waves have been observed in previous theoretical studies, such as active Brownian particles [10,11], moving spots in reaction-diffusion systems [12,13], and filaments in semiconductors [14]. Particlelike waves have also been experimentally observed in a gas discharge system [15,16] and in the oxidation of CO on single-crystal Pt [17].

In this Letter, we generalize the wave front interaction model [2,4] to describe the stabilized wave segments and show how their size depends on the excitability of the medium. These waves are particularly amenable to this analysis because they are stationary in the moving coordinate system. Our analysis offers a theoretical characterization of the separatrix defined by the locus of wave size as a function of excitability, and we show that it is consistent with descriptions of critical fingers.

We use a generic, two-variable reaction-diffusion model for excitable media:

$$\frac{\partial u}{\partial t} = D\nabla^2 u + F(u, v), \quad \frac{\partial v}{\partial t} = \epsilon[G(u, v) + I(t)], \quad (1)$$

where the variables $u(x, y, t)$ and $v(x, y, t)$ represent, respectively, the activator and inhibitor in a two-dimensional reaction medium, and typically $\epsilon \ll 1$. The function $I(t)$

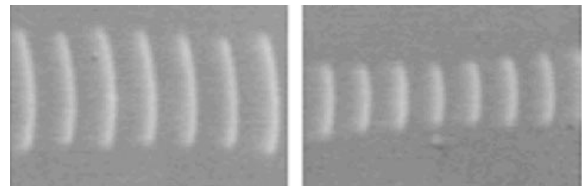


FIG. 1. Stabilized wave segments in the photosensitive BZ reaction. Left and right panels show waves stabilized at lower and higher excitabilities, resulting from higher and lower light intensities, respectively. Superimposed snapshots are shown with an interval of 40.0 s between snapshots; panels ca. 0.95 cm \times 1.45 cm. Figure adapted from Ref. [8].

specifies a feedback parameter, such as the intensity of light imposed on the photosensitive BZ medium, which is applied uniformly over the domain.

For the functions $F(u, v)$ and $G(u, v)$, we take the form used previously [2]:

$$F(u, v) = 3u - u^3 - v, \quad G(u, v) = u - \delta, \quad (2)$$

with the parameter values $D = 1$, $\epsilon = 0.005$, and $\delta = -1.6$. This system has a single uniform rest state, $(u_0, v_0) = (\delta, 3\delta - \delta^3)$, which is stable with respect to small perturbations. However, a suprathreshold perturbation applied to the rest state (or specific initial conditions) gives rise to an undamped, propagating excitation wave.

For $I(t) = I_c \simeq 0.05942$ and these parameters, the excitability of the medium corresponds to the boundary between the excitable and subexcitable medium, where the critical finger is observed. When $I(t) > I_c$, the medium is subexcitable and propagating wave segments contract and disappear. For $I(t) < I_c$, the medium is excitable and propagating wave segments of different sizes, corresponding to different excitabilities, can be stabilized by feedback to the excitability of the medium.

We assume the wave segment propagates in x direction, and we will characterize it by its width (rather than by its area or arc length as in [7,8]). To this end, we follow the location $y_{\max}(t)$ of the tip of the wave along the y axis orthogonal to the propagation direction. The wave is stabilized by negative feedback to the medium excitability with respect to the wave width, where the control parameter $I(t)$ is proportional to the half-width y_{\max} of the wave segment

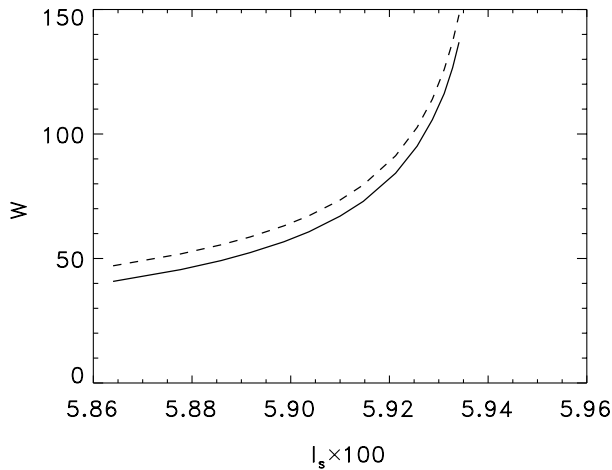


FIG. 2. Width W of stabilized waves as a function of the asymptotic value of the control parameter I_s , computed for the system (1) and (2) subjected to feedback stabilization according to (3) (solid line) and from approximation (22) (dashed line). A computational grid of 500×500 elements was used, comoving with the propagating wave, with time and space steps $\Delta t = 0.02$ and $\Delta x = 0.3$.

$$I(t) = k_{fb}[y_{\max}(t) - y_d] + I_0. \quad (3)$$

Figure 2 shows the results of feedback stabilization over a range of wave widths, with $k_{fb} = 0.00005$, $I_0 = 0.058$, and the target width y_d taken from the interval $28 < y_d < 110$. We see that the wave width, $W \equiv y_{\max}(\infty)$, is a monotonically increasing function of the asymptotic value of the control parameter $I_s \equiv I(\infty)$. The increase in W with I_s is very much like the increase in wave size with increase in light intensity in the photosensitive BZ reaction and in simulations using the Oregonator model [7,8].

A wave segment propagating in a two-dimensional medium can be characterized by the two boundaries that define it: the wave front and the wave back. The problem of wave propagation can be considered as a free-boundary problem, where the normal velocity of the boundary c_n depends on the value of slow variable v at the boundary and on the local interfacial curvature k [18]. At the midpoint of the stabilized wave segment, $y = 0$, the normal direction coincides with the propagation direction of the full wave along the x axis, as shown in Fig. 3. Let Θ^+ (Θ^-) specify the angle between the x axis and the outward (inward) pointing normal on the front (back) boundary and s^+ (s^-) be the arc length measured from the top of the stabilized segment. Then the normal velocity of the front and of the back should be written as $c_n^+ = c(v^+) - Dk^+$ and $c_n^- = -c(v^-) - Dk^-$, where the local curvature of the front (back) is expressed as

$$k^\pm = -d\Theta^\pm/ds^\pm. \quad (4)$$

Let k_m be the local curvature at the midpoint of the stabilized wave. The propagation velocity of the wave is therefore $c_s = c_0 - Dk_m$, where $c_0 = c(v^+) = c(v_0)$.

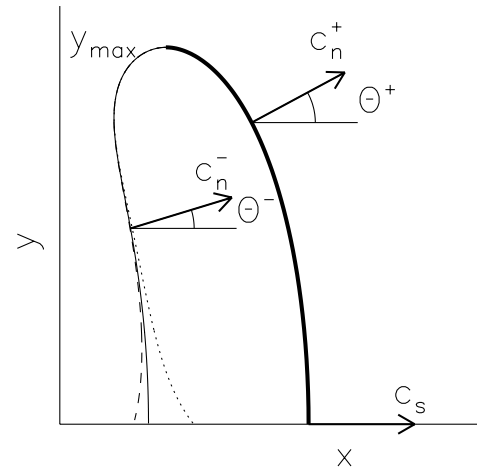


FIG. 3. Boundaries of a propagating wave segment computed as the solution of the free-boundary problem (5)–(7) for $K_m = 0.0402$ and $B_k = 0.5108$. The wave front (back) is shown by a thick (thin) solid line. Solutions computed for slightly deviated values $B_k = 0.5101$ and $B_k = 0.5110$ are shown by dotted and dashed lines, respectively.

Note that within the excited region $u = u_e(v)$, where $u_e(v)$ is the largest root of equation $F(u, v) = 0$. Then the free-boundary problem for the stabilized wave segment can be written as

$$c_0 - Dk^+ = c_s \cos(\Theta^+), \quad (5)$$

$$-c(v^-) - Dk^- = c_s \cos(\Theta^-), \quad (6)$$

$$c_s dv/dx = -\epsilon[G(u_e(v), v) + I_s]. \quad (7)$$

Equations (5) and (6) describe the geometry of the front and back of the wave, respectively, while Eq. (7) describes the evolution of the slow variable v between the front and the back of the wave.

Using Eq. (4), one can transform Eq. (5) into an ordinary differential equation for the angle Θ^+ :

$$D \frac{d\Theta^+}{ds^+} = c_s \cos(\Theta^+) - c_0. \quad (8)$$

Since $dy^+ = -ds^+ \cos(\Theta^+)$ and $dx^+ = ds^+ \sin(\Theta^+)$, it is straightforward to obtain equations for the Cartesian coordinates (x^+, y^+) of the front [7,19]:

$$\frac{dx^+}{d\Theta^+} = \frac{D \sin(\Theta^+)}{c_s \cos(\Theta^+) - c_0}, \quad (9)$$

$$\frac{dy^+}{d\Theta^+} = -\frac{D \cos(\Theta^+)}{c_s \cos(\Theta^+) - c_0}. \quad (10)$$

For the conditions $x^+ = 0$, $\Theta^+ = \pi/2$ and $y^+ = 0$, $\Theta^+ = 0$, the solutions of Eqs. (9) and (10) have the form

$$\frac{x^+}{D} = \frac{1}{c_s} \ln \frac{c_0}{c_0 - c_s \cos(\Theta^+)}, \quad (11)$$

$$\frac{y^+}{D} = -\frac{\Theta^+}{c_s} + \frac{2c_0}{c_s \sqrt{c_0^2 - c_s^2}} \arctan \frac{(c_0 + c_s) \tan \frac{\Theta^+}{2}}{\sqrt{c_0^2 - c_s^2}}. \quad (12)$$

These expressions specify the shape of the wave front, $x^+ = x^+(y^+)$, for any k_m within the interval $0 < k_m < c_0/D$.

In order to obtain the shape of the wave back, the function $c = c(v)$ must be specified. We first assume this monotonically decreasing function vanishes at a value $v = v^*$. We can then say, in the vicinity of v^* , the wave velocity is a linear function of v : $c(v) = \alpha(v^* - v)$. The constant α is uniquely determined by $F(u, v^*)$. For the case we consider here, where $F(u, v^*)$ is the cubic function of u defined in Eq. (2), $\alpha = 1/\sqrt{2}$ [2]. We follow Karma [2] and introduce the quantity $\Delta = v^* - v_0$, which characterizes the excitability of the medium. Note that the propagation velocity can be written as $c_0 = \alpha\Delta$, provided that $\Delta \ll 1$. For $\epsilon \ll 1$, we can use the approximation $G[u_e(v), v] + I_s = G^*$, where $G^* = G[u_e(v^*), v^*] + I_s$ [2]. With this approximation, the value of the slow variable at the wave back v^- can be obtained from Eq. (7):

$$v^- = v_0 + \frac{G^* \epsilon}{c_s} [x^+(y) - x^-(y)]. \quad (13)$$

Substitution of Eq. (13) into Eq. (6) results in an equation for the back of the wave

$$D \frac{d\Theta^-}{ds^-} = c_0 - \frac{G^* \epsilon \alpha}{c_s} (x^+ - x^-) + c_s \cos(\Theta^-). \quad (14)$$

After rescaling of space ($S^- = c_0 s^-/D$, $X^\pm = c_0 x^\pm/D$, and $K_m = Dk_m/c_0$), Eq. (14) becomes

$$\frac{d\Theta^-}{dS^-} = 1 - \frac{B_k(X^+ - X^-)}{(1 - K_m)} + (1 - K_m) \cos(\Theta^-), \quad (15)$$

where

$$B_k = \frac{G^* D \epsilon}{\alpha^2 \Delta^3}. \quad (16)$$

In order to integrate this equation we rewrite Eqs. (11) and (12) in dimensionless form and fix $0 < K_m < 1$. Numerical integration of Eq. (15) starting with $\Theta^- = -\pi/2$, $X^- = 0$, and $Y^- = Wc_0/D$ at $S^- = 0$, and taking into account that $dY^-/dS^- = -\cos(\Theta^-)$ and $dX^-/dS^- = \sin(\Theta^-)$, produces a solution depending on B_k . Using a trial and error method one must vary the value of B_k until the corresponding solution satisfies the second boundary condition, $Y^- = 0$, $\Theta^- = 0$ (see Fig. 3). Repetition of this process for different K_m yields the dependence $B_k = B_k(K_m)$ shown in Fig. 4. For $K_m \ll 1$ this dependence is well approximated by the linear relationship

$$B_k = B_0 - \beta \frac{Dk_m}{c_0}, \quad (17)$$

where $\beta = 0.63$. We note that for $K_m = 0$, the wave segment is identical to the critical finger studied in Refs. [2,4], and the value of $B_k(K_m \rightarrow 0)$ computed for the free-boundary problem (5)–(7) coincides with the value $B_0 = 0.535$ found for the critical finger [2].

Since our ultimate goal is to explain the relationship between the width of the wave segment W and the control parameter I_s , it is convenient to rewrite Eq. (17) as

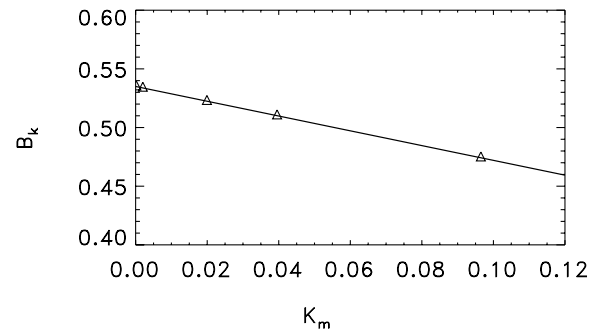


FIG. 4. Function $B_k = B_k(K_m)$ obtained from numerical analysis of Eq. (15).

$$\frac{Dk_m}{c_0} = \frac{1}{\beta}(B_0 - B_k). \quad (18)$$

The value k_m determines the width of the wave segment W in accordance with Eq. (12) after the substitution $\Theta^+ = \pi/2$. In the case of small curvature ($Dk_m/c_0 \ll 1$), this relationship is given by the expression (cf. [7,8])

$$W^2 = \frac{\pi^2 D}{2c_0 k_m}. \quad (19)$$

Substitution of Eq. (18) into Eq. (19) results in the important relationship

$$\frac{D^2}{W^2 c_0^2} = \frac{2}{\beta \pi^2} (B_0 - B_k). \quad (20)$$

Thus, if the control parameter I_s influences the value of B_k , it determines the value of k_m and, in turn, the width of the wave segment. If the control parameter I_s differs only slightly from the value I_c , corresponding to the critical finger, i.e., $I_c - I_s \ll I_c$, Eq. (20) can be linearized to give

$$\frac{D^2}{W^2 c_0^2} = \frac{2}{\beta \pi^2} \left. \frac{dB_k}{dI_s} \right|_{I_s=I_c} (I_c - I_s). \quad (21)$$

In order to obtain quantitative results for the reaction-diffusion model (1) and (2), note that the quantities G^* and Δ in Eq. (16) depend on the control parameter I_s and can be expressed as $G^* = \sqrt{3} - \delta + I_s$ and $\Delta = (\delta - I_s)^3 - 3(\delta - I_s)$, since $v^* = 0$. Thus, for the model under consideration Eq. (21) can be written as

$$\frac{D^2}{W^2 c_0^2} = \frac{2B_0}{\beta \pi^2} \left(\frac{9[(\delta - I_c)^2 - 1]}{\Delta_c} + \frac{1}{G_c^*} \right) (I_c - I_s). \quad (22)$$

Here values Δ_c and G_c^* correspond to $I_s = I_c$. The computed propagation velocity of the stabilized wave is $c_0 = 0.277$. Substituting this value into Eq. (22), we find the width W of the wave segment as a function of I_s , as shown in Fig. 2. The dashed line, showing the theoretical result, is in excellent agreement with the direct integration of the reaction-diffusion model (1)–(3), shown by the solid line.

In summary, the existence of stabilized propagating wave segments can be understood by considering the interaction of the wave front and wave back boundaries. We note that relationship (17) is universal, as it contains only the general characteristics of the two-component model (1). It also describes the limiting case of the critical finger [2] when the size of the wave segment goes to infinity. Equation (21) is also general, since the way in which the control parameter I_s influences the parameter B_k is not explicitly specified. In particular, it provides a qualitative explanation for the similar linear relationships obtained in

experiments with the light-sensitive BZ reaction and for the Oregonator model [7,8].

Equation (22) demonstrates how these universal results can be applied to a specific model of excitable media. A comparison of the theoretical predictions with the direct numerical integration (see Fig. 2) shows that there is good quantitative agreement even for the case where ϵ is not extremely small. Therefore, the theoretical approach developed here provides the opportunity to test quantitative studies of propagating wave segments in a variety of different active media.

We thank the National Science Foundation (CHE-0415392), the Office of Naval Research, the Deutsche Forschungsgemeinschaft (SFB 555), and the Alexander von Humboldt Foundation for supporting this research. K. S. thanks Alexander Mikhailov for helpful discussions and his hospitality at the Fritz-Haber-Institut der Max-Planck-Gesellschaft.

-
- [1] P. Pelce and J. Sun, *Physica D* (Amsterdam) **48**, 353 (1991).
 - [2] A. Karma, *Phys. Rev. Lett.* **66**, 2274 (1991).
 - [3] A. S. Mikhailov and V. S. Zykov, *Physica D* (Amsterdam) **52**, 379 (1991).
 - [4] V. Hakim and A. Karma, *Phys. Rev. E* **60**, 5073 (1999).
 - [5] A. N. Zaikin and A. M. Zhabotinsky, *Nature* (London) **225**, 535 (1970).
 - [6] L. Kuhnert, *Nature* (London) **319**, 393 (1986).
 - [7] E. Mihaliuk, T. Sakurai, F. Chirila, and K. Showalter, *Faraday Discuss.* **120**, 383 (2001).
 - [8] E. Mihaliuk, T. Sakurai, F. Chirila, and K. Showalter, *Phys. Rev. E* **65**, 065602(R) (2002).
 - [9] T. Sakurai, E. Mihaliuk, F. Chirila, and K. Showalter, *Science* **296**, 2009 (2002).
 - [10] F. Schweitzer, W. Ebeling, and B. Tilch, *Phys. Rev. Lett.* **80**, 5044 (1998).
 - [11] U. Erdmann, W. Ebeling, L. Schimansky-Geier, and F. Schweitzer, *Eur. Phys. J. B* **15**, 105 (2000).
 - [12] K. Krischer and A. Mikhailov, *Phys. Rev. Lett.* **73**, 3165 (1994).
 - [13] C. P. Schenk, M. Or-Guil, M. Bode, and H.-G. Purwins, *Phys. Rev. Lett.* **78**, 3781 (1997).
 - [14] M. Gaa and E. Schöll, *Phys. Rev. B* **54**, 16733 (1996).
 - [15] I. Brauer, M. Bode, E. Ammelt, and H.-G. Purwins, *Phys. Rev. Lett.* **84**, 4104 (2000).
 - [16] C. Strümpel, H.-G. Purwins, and Yu. A. Astrov, *Phys. Rev. E* **63**, 026409 (2001).
 - [17] M. Bertram, C. Beta, M. Pollmann, A. S. Mikhailov, H. H. Rotermund, and G. Ertl, *Phys. Rev. E*, **67**, 036208 (2003).
 - [18] J. J. Tyson and J. P. Keener, *Physica D* (Amsterdam) **32**, 327 (1988).
 - [19] O. Steinbock, V. S. Zykov, and S. C. Müller, *Phys. Rev. E*, **48**, 3295 (1993).